

Supporting Information for  
Pressure Effect on the Magnetism and Crystal Structure of  
Magnetoelectric Metal-Organic Framework  $[\text{CH}_3\text{NH}_3][\text{Co}(\text{HCOO})_3]$

Houjian Zhou<sup>a</sup>, Hao Ding<sup>a</sup>, Xin Gao<sup>a</sup>, Zhiwei Shen<sup>a</sup>, Kun Zhai<sup>\*a</sup>, Bochong Wang<sup>a</sup>, Congpu Mu<sup>a</sup>, Fusheng Wen<sup>a</sup>, Jianyong Xiang<sup>a</sup>, Tianyu Xue<sup>a</sup>, Yu Shu<sup>\*a</sup>, Lin Wang<sup>a</sup>, Zhongyuan Liu<sup>\*a</sup>

Table S1 The crystallographic information of refined crystal structure

Empirical formula	$\text{C}_4\text{H}_9\text{CoNO}_6$
Formula weight	226.05
Temperature [K]	300
Crystal system	orthorhombic
Space group (number)	<i>Pnma</i> (62)
<i>a</i> [ $\text{\AA}$ ]	8.39295(16)
<i>b</i> [ $\text{\AA}$ ]	11.70918(20)
<i>c</i> [ $\text{\AA}$ ]	8.10619(17)
$\alpha$ [ $^\circ$ ]	90.0
$\beta$ [ $^\circ$ ]	90.0
$\gamma$ [ $^\circ$ ]	90.0
Volume [ $\text{\AA}^3$ ]	796.633(26)
<i>Z</i>	4
Radiation	$\lambda = 1.540562 \text{\AA}$

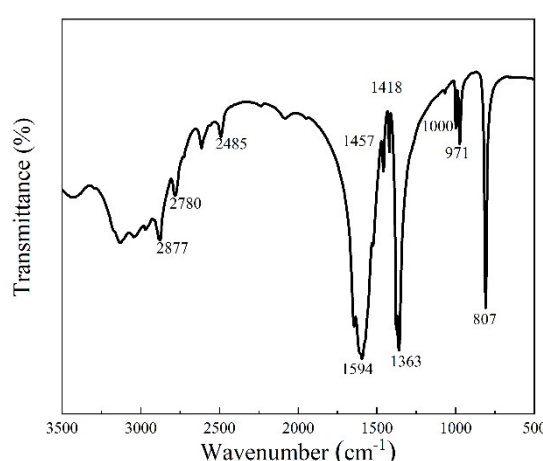


Figure S1 the Infrared spectrum of the  $[\text{CH}_3\text{NH}_3][\text{Co}(\text{COOH})_3]$  compound recorded at room temperature.

Table S2 Experimental IR and Raman wavenumbers (in  $\text{cm}^{-1}$ ) of  $[\text{CH}_3\text{NH}_3][\text{Co}(\text{COOH})_3]$  and suggested assignments.

$[\text{CH}_3\text{NH}_3][\text{Co}(\text{HCOO})_3]$		Assignment
IR	Raman	
3121vw		$\nu(\text{N} - \text{H})$
	3051w	$\nu(\text{NH}_3^+) + \nu(\text{CH}_3)$
3031vw		$\nu(\text{N} - \text{H})$
	2979s	$\nu(\text{CH}_3)$
2963w		$\nu(\text{CH}_3)$
	2903m	$\nu_1(\text{HCOO}^-)$
	2893m	$\nu_1(\text{HCOO}^-)$
2882w	2879m	$\nu_1(\text{HCOO}^-)$
	2826w	$\nu(\text{NH}_3^+)$
2779w		$\nu(\text{C} - \text{H})$
	2726vw	
2614w		$\nu(\text{NH})$
2489w		$\nu(\text{NH})$
	1646w	$\nu_4(\text{HCOO}^-) + \delta_{\text{as}}(\text{NH}_3^+)$
	1611w	
	1577w	$\nu_4(\text{HCOO}^-)$
	1514w	
	1464w	$\delta_s(\text{NH}_3) + \delta_{\text{as}}(\text{CH}_3)$
1457m		$\nu(\text{CH}_3)$
1418m	1422w	$\delta_s(\text{CH}_3)$
	1380vs	$\nu_5(\text{HCOO}^-)$
	1373vs	$\nu_5(\text{HCOO}^-)$
	1368vs	$\nu_5(\text{HCOO}^-)$
1357s	1388vs	$\nu_2(\text{HCOO}^-)$
1068vw	1066m	$\nu_6(\text{HCOO}^-)$
1000m	998m	$\nu(\text{C} - \text{N})$
973m	972vw	$\nu(\text{C} - \text{N})$
807s	807m	$\nu_3(\text{HCOO}^-)$
	803m	$\nu_3(\text{HCOO}^-)$

Key: vs, very strong; s, strong; m, medium; w, weak; vw, very weak.

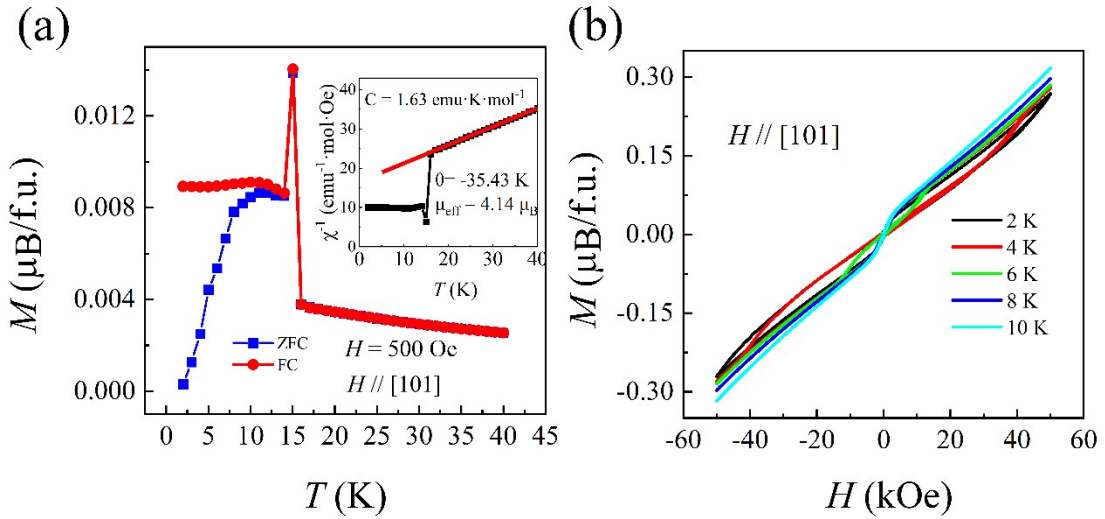


Figure S2 (a) Magnetization as a function of temperature along [101] axis after zero-field cooling (ZFC) and field cooling (FC) process. (b) Field-dependent isothermal magnetization along [101] axis at different temperatures.

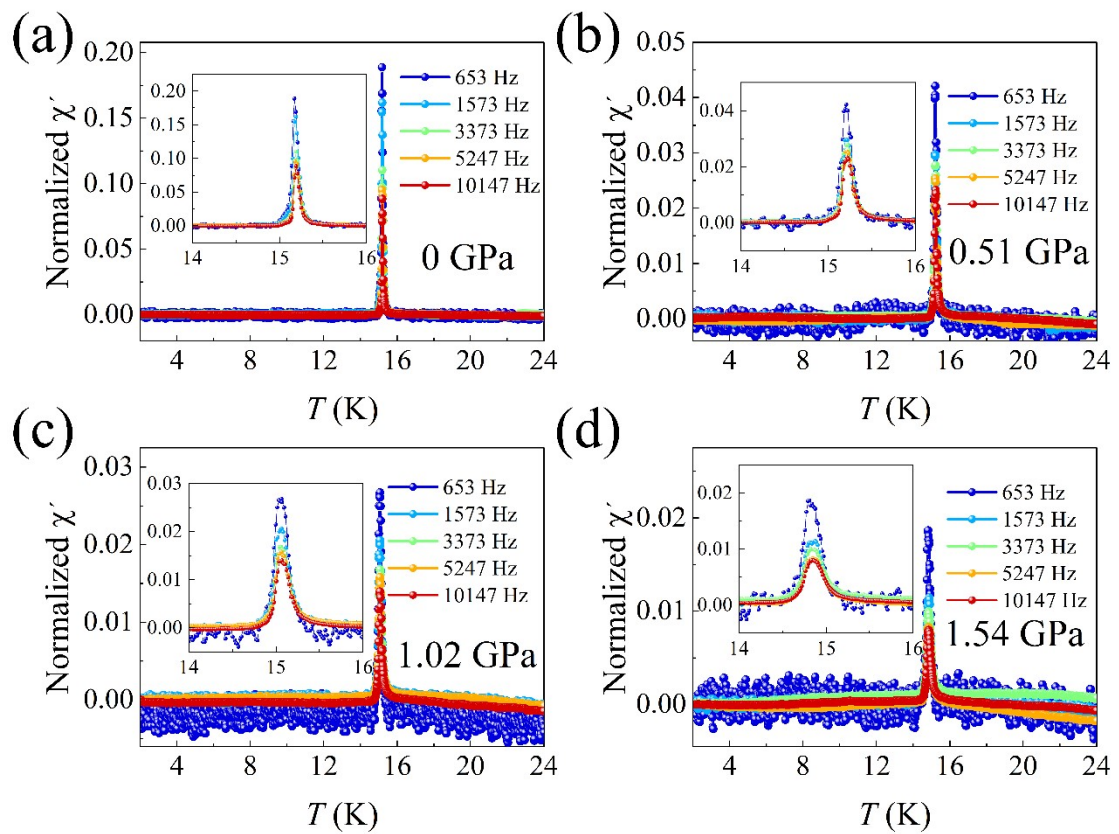


Figure S3 Normalized AC magnetic susceptibility at different frequencies under different pressures of (a) 0GPa, (b) 0.51GPa, (c) 1.02GPa and (d) 1.54GPa.

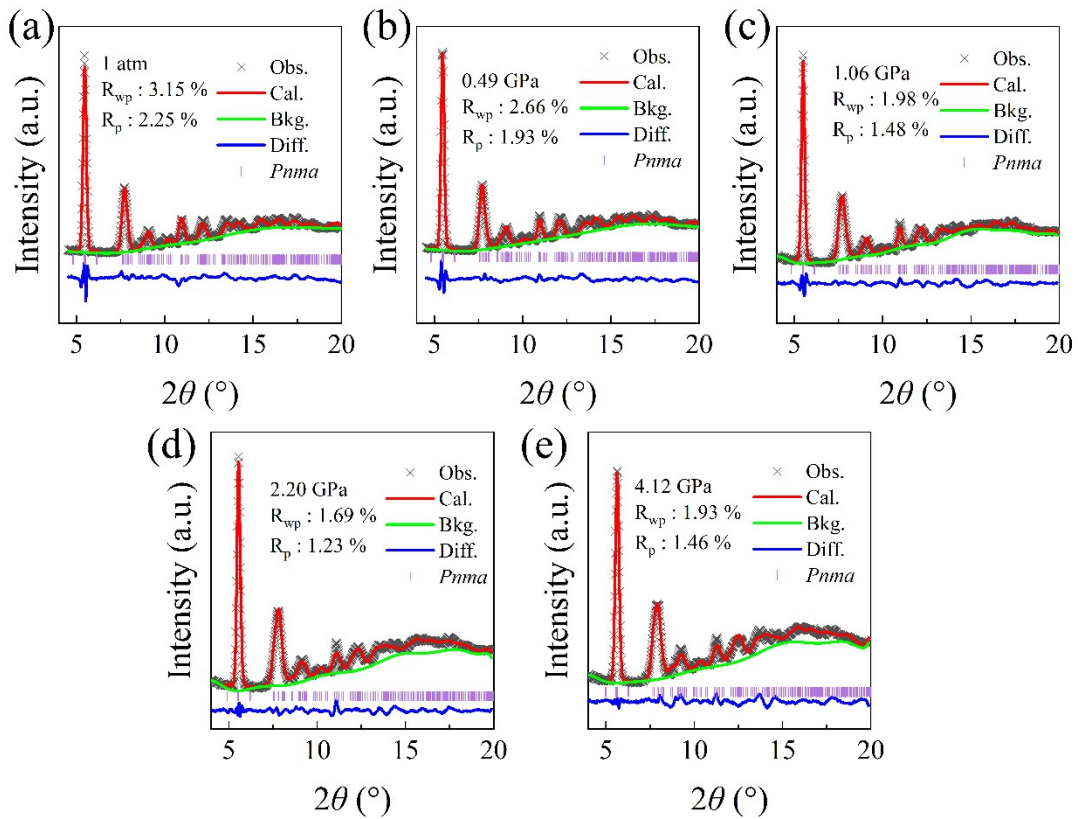


Figure S4 Rietveld refinement of powder XRD patterns at (a) 0, (b) 0.49, (c) 1.60, (d) 2.20, and (e) 4.12 GPa with the *Pnma* space group using the GSAS software.

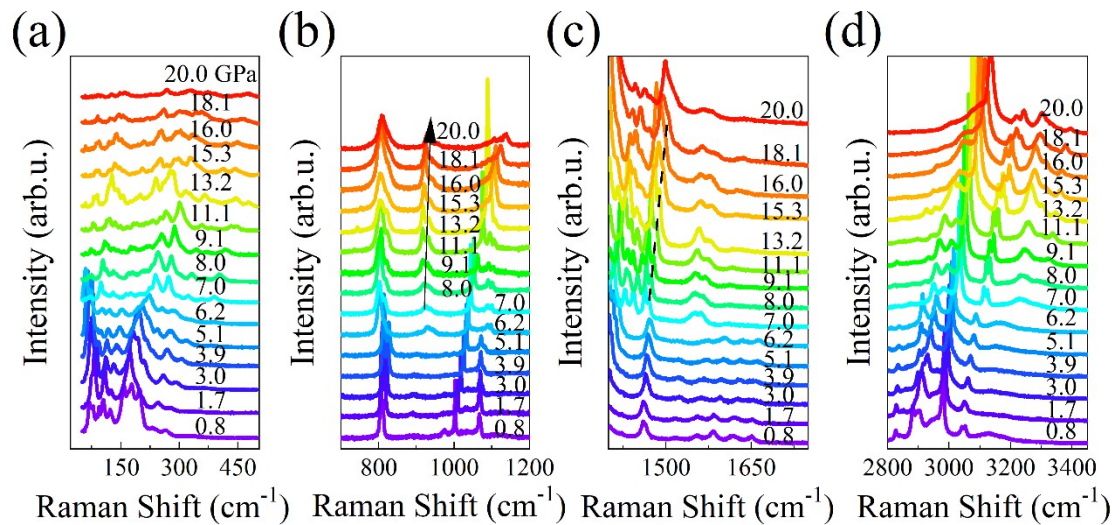


Figure S5 Raman spectra of  $[\text{CH}_3\text{NH}_3]\text{[Co}(\text{COOH})_3]$  single crystal at high pressures in the wavenumber of (a) 50-500  $\text{cm}^{-1}$ , (b) 700-1200  $\text{cm}^{-1}$ , (c) 1400-1700  $\text{cm}^{-1}$ , (d) 2700-3500  $\text{cm}^{-1}$ .

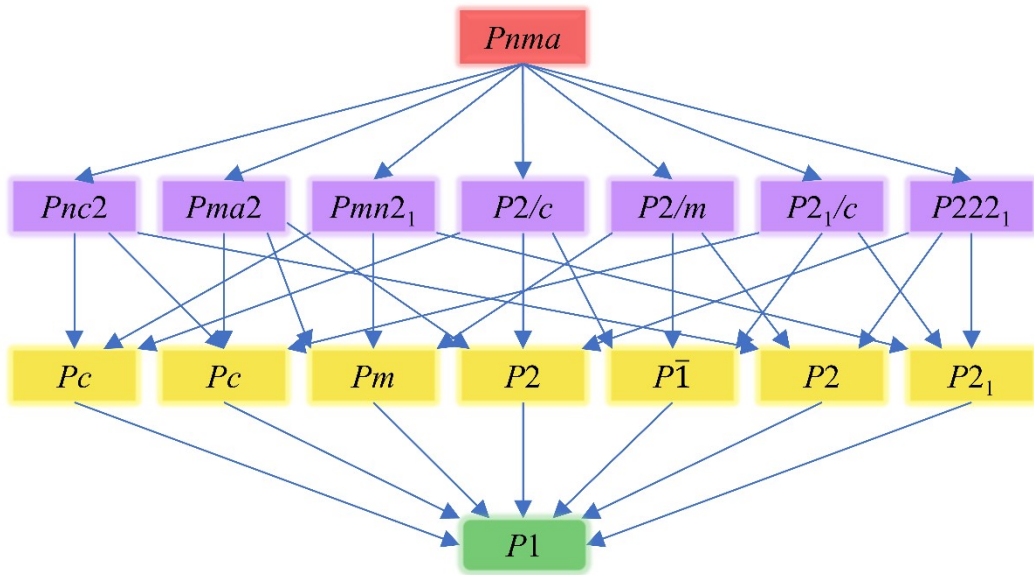


Figure S6 Schematic representation of the subgroup tree.

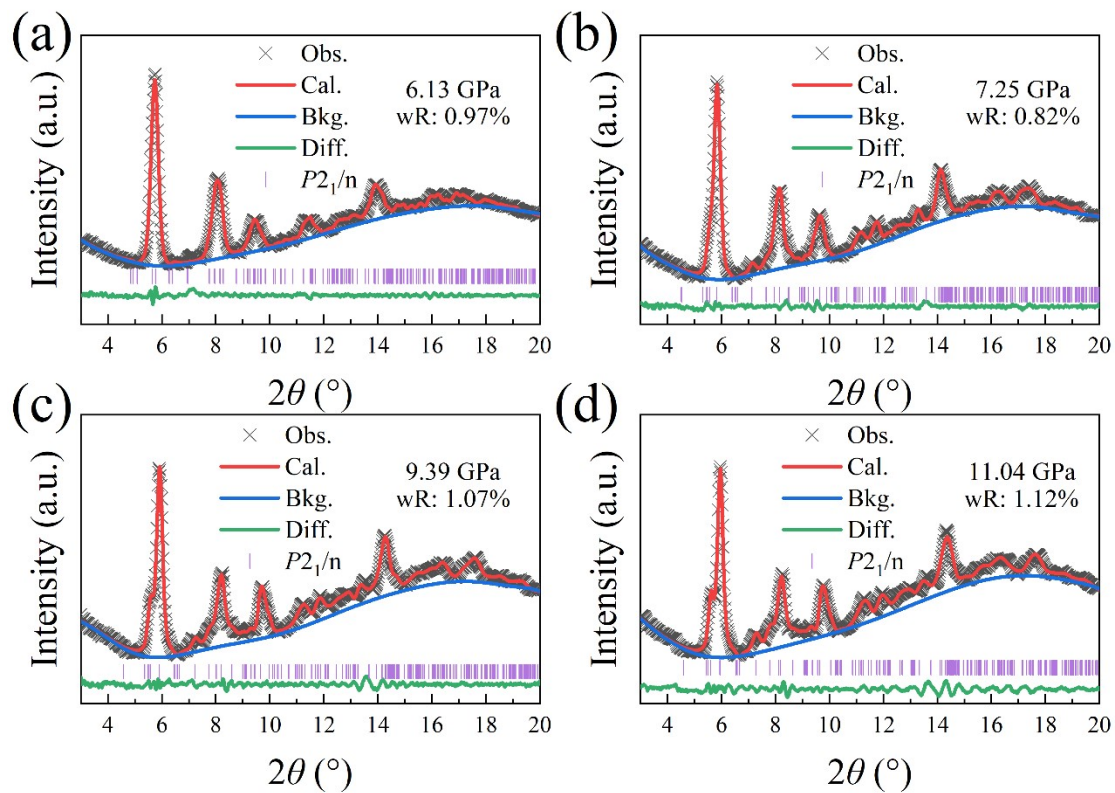


Figure S7 Refinement of powder XRD patterns at (a) 6.1, (b) 7.3, (c) 9.4 and (d) 11.0 GPa by the GSAS II software.

Table S3 Pressure evolution of the bond-length and bond angles of  $[\text{CH}_3\text{NH}_3][\text{Co}(\text{COOH})_3]$ .

	0	0.49	1.06	2.20	4.12	6.13	7.25	9.39	11.04
Bond Length (Å)									
C-O	1.47	1.46006	1.46625	1.47463	1.44262	1.22164	1.21615	1.21861	1.20388
	1.83	1.83276	1.8285	1.83431	1.79419	1.20095	1.20468	1.20937	1.20938
	1.48	1.47689	1.47138	1.47416	1.44197	1.2492	1.30602	1.29744	1.29234
Co-O						1.23437	1.13502	1.12973	1.11697
						1.23996	1.28636	1.2781	1.26758
						1.22199	1.12378	1.11955	1.11649
						2.02201	2.00391	2.00767	1.98267
						2.03631	1.9154	1.90998	1.9079
O-C-O	1.66	1.65711	1.64712	1.6469	1.61101	2.09648	2.2197	2.2038	2.194
	2.21	2.21	2.2018	2.2038	2.15588	2.02853	1.89369	1.88576	1.86275
						2.02781	2.02248	2.0296	2.03045
Bond Angle (°)									
O-C-O	122	121.416	122.066	122.234	122.259	123.298	129.969	130.363	130.409
						124.392	123.457	123.224	123.51
						125.219	123.832	123.5	123.153